Microchemical Journal 225 (2026) 118027

Contents lists available at ScienceDirect

Microchemical Journal

journal homepage: www.elsevier.com/locate/microc

Near-infrared (NIR) spectroscopy for quantitative modelling of quaternary microplastic mixtures and the effect of interferents

Enmanuel Cruz Muñoz [a], Claudio Marchesi [b], Mario Rigo [b], Sundus Ali [b], Laura Eleonora Depero [b], Giuseppe Andrea de Lucia [c], Andrea Camedda [c], Silvia Prati [d], Davide Ballabio [a], Giorgia Sciutto [d,*], Stefania Federici [b,*]

[a] Department of Earth and Environmental Sciences, University of Milano-Bicocca, Piazza Della Scienza 1, 20126 Milano, Italy
[b] Chemistry for Technologies Laboratory, Department of Mechanical and Industrial Engineering, University of Brescia & INSTM RU of Brescia, Via Branze, 38, 25123 Brescia, BS, Italy
[c] Institute of Anthropic Impact and Sustainability in marine Environment - National Research Council Località Sa Mardini, 09170 Torregrande, Oristano, Italy
[d] Department of Chemistry "G. Ciamician", University of Bologna, Ravenna Campus, Via Guaccimanni 42, Ravenna, Italy

ARTICLE INFO

Keywords:
Microplastic quantification
Near-infrared spectroscopy (NIR)
Chemometrics
Environmental interferents
Partial least squares regression (PLS)

ABSTRACT

The detection and quantification of microplastics (MPs) in environmental samples remain a significant analytical challenge due to the heterogeneity of polymer mixtures and the presence of organic and inorganic interferents. While Near-infrared (NIR) spectroscopy has emerged as a rapid, cost-effective alternative, most studies have focused on qualitative detection or simplified systems, leaving the influence of environmental interferents largely unexplored. This study proposes a quantitative analytical strategy using a portable NIR spectrometer combined with multivariate regression for the determination of four target polymers (polypropylene, PP, polyethylene, PE, polystyrene, PS, and polyethylene terephthalate, PET) in complex mixtures. MPs were generated through a true-to-life protocol, ensuring realistic particle morphologies and surface conditions. Model robustness was systematically assessed against a wide range of environmental interferents, including non-target polymers (polyvinyl chloride, polylactic acid, and polyamide), natural fibres (cotton, silk), vegetal material, and mineral particles ($CaCO_3$). Polymer quantification was performed through Partial Least Squares (PLS) regression, with each polymer modelled independently. The proposed modelling approach was subjected to a double cross-validation procedure, and their predictive ability was further estimated by external validation procedure. In particular, when external validation samples were spiked with interferents, prediction errors increased moderately due to added spectral complexity; however, the models maintained satisfactory performance, with PE and PET demonstrating the greatest resilience to matrix effects. Finally, the models were successfully applied for the quantification in real environmental samples, with a satisfactory accuracy considering the inherent complexity of "unknown" environmental matrices. These results demonstrate the potential of portable NIR spectroscopy and robust chemometric modelling for quantitative MP analysis in heterogeneous, environmentally realistic scenarios.

1. Introduction

The widespread presence of microplastics (MPs), defined by ISO/TR 21960:2020 as plastic particles from 1 μm to 1 mm (and up to 5 mm for larger MPs) [1], poses a serious environmental threat, with potential ecological, economic, and social impacts [2–6]. MPs have emerged as a major environmental concern due to arise from two main sources: primary MPs, intentionally manufactured at small sizes (e.g., industrial pellets, cosmetic microspheres), and secondary MPs, formed through the degradation of larger items by physical, chemical, or biological processes [7–10].

The reliable identification and quantification of MPs in ecosystems still face significant methodological challenges, mainly due to the high physicochemical heterogeneity (in terms of the size, shape and polymer composition) of polymer mixtures and the simultaneous presence of organic and mineral interferents. In addition, the long analysis times and

* Corresponding authors.
E-mail addresses: giorgia.sciutto@unibo.it (G. Sciutto), stefania.federici@unibs.it (S. Federici).

https://doi.org/10.1016/j.microc.2026.118027
Received 2 February 2026; Received in revised form 31 March 2026; Accepted 9 April 2026
Available online 11 April 2026

high costs often hinder adequate sampling replication, limiting an accurate assessment of MPs abundance and composition at a global scale.

A variety of analytical techniques have been proposed for detecting MPs in environmental samples [11]. Among other, spectroscopic single-point techniques have become key tools for MPs characterization. In particular, Fourier-Transform Infrared (FTIR) and Raman micro spectroscopy are currently the most widely employed approaches for the qualitative identification of MPs, owing to their ability to provide characteristic molecular fingerprints [12,13]. These methods are now recognized as reference analytical tools in the field and are included in international standardization efforts that formally define procedures for the application of vibrational spectroscopy for MP analysis [14]. However, when operated in micro-spectroscopic modes both FTIR and Raman spectroscopies are typically restricted by relatively long analysis times and by the need for expensive instrumentation, limiting their use in large-scale monitoring or *on-site* investigations [15,16]. The development and application of cost-effective analytical methods for detecting MPs across different environmental compartments are currently stated as a research priority for assessing the risks associated with MPs contamination.

Whitin this scenario, Near-Infrared (NIR) spectroscopy is gaining increasing attention as a complementary and more operationally flexible approach [17–19]. NIR spectroscopy offers several advantages: it is rapid, non-destructive, and can be applied directly to bulk or unprepared samples, making it particularly suitable for high-throughput on-field screening applications [20].

Piarulli et al. first proposed near-infrared hyperspectral imaging (NIR-HSI) as a fast and cost-efficient technique for detecting MPs directly on filters, without extensive purification or handling steps [21]. NIR-HSI has become an increasingly popular technique, with several studies demonstrating its applicability for MP detection in environmental matrices [22].

However, despite these advantages, the potential of the method remain partially underexplored and has so far been limited mainly to qualitative applications, as quantitative NIR analysis still faces several challenges, such as the broad and overlapped absorption bands, the variability introduced aging processes, particle morphology, and presence of interferents [23].

Marchesi et al. provided a preliminary assessment of NIR spectroscopy for quantitative analysis using simplified ternary polymer mixtures (polypropylene PP, polystyrene PS, and polyethylene PE), but without evaluating the impact of interferents. While this work represents a first step toward addressing real-world complexity, the absence of interferents still constitutes a significant simplification compared to actual environmental scenarios [24].

In the present study, an analytical method based on the use of a portable NIR spectrometer in combination with multivariate regression is proposed for the quantification of components in four-polymer mixtures, under conditions that closely resemble those encountered in marine and terrestrial environmental matrices. To this aim, MPs obtained from four polymers (PP, PS, PE, and polyethylene terephthalate PET) were prepared using a true-to-life fragmentation protocol designed to mimic realistic particle morphologies and surface conditions. The selection of the target polymers was based on their well-documented prevalence in environmental samples [25–27], where they are consistently reported as the most abundant MPs, to develop and evaluate the model on the most environmentally relevant materials. The addition of PET in the investigated polymer mixtures is particularly relevant in this context. Due to its extensive use in packaging and textiles, PET is one of the most abundant polymers found in the environment [28,29]. Incorporating PET into multicomponent models not only increases the environmental representativeness of the mixtures, but also introduces new analytical challenges linked to its different absorption features: since PET exhibits distinct chemical and optical properties compared to the polymers typically included in previous NIR studies.

Moreover, to further assess the robustness of the method, the influence of several interferents, representing both organic and inorganic interferents, including additional polymers (polyvinyl chloride, PVC, polylactic acid, PLA, and polyamide 66, PA66), natural fibres (cotton, silk), vegetal materials (leaves, wood), and mineral particles ($CaCO_3$) was critically evaluated. In fact, environmental samples usually contain a complex mixture of polymers and non-plastic materials, which introduces additional spectral interferences and may affect both interpretation and quantitative analysis [30]. Such components can obscure characteristic spectral features of plastics, altering the signal baseline and reducing the reliability of quantitative predictions.

To further bridge the gap between controlled laboratory conditions and real-world scenarios, the proposed modelling approach was also applied to environmental samples collected from coastal areas in Sardinia (Italy). The inclusion of field samples provides an additional level of validation, allowing the assessment of model performance in the presence of naturally aged MPs and complex, unknown matrices. This step is essential to demonstrate the practical applicability of the method beyond synthetic mixtures and to evaluate its reliability as a screening tool under realistic environmental conditions.

2. Material and methods

The workflow adopted in this study comprises the generation of true-to-life MPs, the preparation of mixtures for model calibration and external validation, spectral acquisition, and data analysis. An overview of these phases is provided in the schematic summary in the Supplementary Material (**Fig. S1**), and each step is described in detail in the following sections.

2.1. True-to-life approach for the generation of microplastics

Secondary MPs were produced at the laboratory scale following the protocol previously reported for ternary mixtures to produce true-to-life MPs [24], briefly summarized here with minor adaptations introduced to include PET. Commercial day-to-day items were selected as polymer sources: chewing gum bottles (high-density polyethylene, HDPE), single-use beverage glasses (PP), disposable cutlery (PS), and transparent beverage bottles (PET). After removal of printed areas, the materials were washed, cut, embrittled in liquid nitrogen, and mechanically fragmented under wet-grinding conditions using an immersion blender. The resulting suspensions were dried at room temperature and sieved through a 500 μm stainless-steel mesh to obtain the target MP fraction. Full procedural details are provided in **Section S1** of the Supplementary material.

2.2. Mixtures preparation for model calibration

True-to-life MP samples were prepared according to the percentage content of each polymer, starting from 0 to 100%, in increments of 10%. In total, 89 samples were prepared: 4 samples were composed by pure substances, 17 were binary mixtures, 10 were ternary mixtures and 58 quaternary mixtures. The composition of the samples included in the calibration set is provided as a table in the supplementary material (**Table S1**).

2.3. Mixtures preparation for external validation set

A new set of true-to-life MPs was prepared to generate an external validation set for model validation, following our previously published protocol with specific adaptations for the selected polymers [31]. Four polymers were selected from different commercial products to ensure chemical and morphological variability compared to the materials used for model calibration: PS from a blue disposable plate, PP from green food packaging, HDPE from laboratory plasticware, and PET from beverage bottles of different brands. Selected items made of PS, PP, HDPE, and PET were cleaned, cut into small fragments, cryogenically

embrittled, and mechanically fragmented using a mixer mill (MM400, Retsch GmbH, Germany). The resulting powders were sieved through a 500 μm mesh to obtain the target MP fraction. Full experimental details are provided in the Supplementary Information (**Section S2**).

Ten samples were prepared by varying the relative mass fractions of the four polymers to cover a broad range of compositions, as reported in **Table S2**, and constituted the external validation set. These samples included the four pure polymers (100% of a single component), one mixture with equal parts of all polymers (25% each), four asymmetric combinations where one polymer was present at a higher percentage (40%) while the others were balanced at lower levels (20%) and one sample with PS and PP at 30% and the other two polymers at 20%.

2.4. Addition of interferents to the external validation set

Three additional polymers were selected to evaluate the effect of interferents: PVC from badge holders, PLA from disposable drinking cups, and PA66 from a white cloth fabric. These materials were fragmented following the same mechanical protocol described for the external validation dataset in **Section 2.3**, using the mixer mill.

In addition to the synthetic polymers, several non-plastic interferents were also included to simulate common sources of environmental contamination. These consisted of natural fibres (cotton and silk obtained from natural organic cloths), organic and vegetal materials (dried leaves and wood pieces obtained from natural environments), and an inorganic component (calcium carbonate, $CaCO_3$, Sigma Aldrich). All materials were ground and sieved under controlled conditions to achieve particle size distributions similar to the MP powders, ensuring comparable scattering behavior during NIR measurements.

The interferents constituted by the additional polymers (PVC, PLA and PA66) and non-plastic materials were subsequently added to samples of the external validation set, prepared according to **Section 2.3**. Each contaminated sample was obtained by mixing the original 100 mg of MP with a total of 20 mg of interferents, corresponding to approximately 5 mg for each class of interferent (polymeric, vegetal, fibrous, and inorganic). This resulted in final samples of 120 mg. The relative proportions of the four polymers were recalculated accordingly to preserve their original mass ratios while accounting for the additional non-plastic material. These ten samples with interferents constituted the spiked external validation set.

2.5. Environmental sample collection and preparation

Environmental samples were collected from surface coastal waters at four sites in Sardinia (Italy), Castelsardo, Sinis, Teulada, and Capo Caccia, selected to represent different coastal environments and potential sources of MP contamination, using a manta trawl net in accordance with the standardized coast–offshore transect methodology adopted within the Italian Marine Strategy monitoring programme [32]. Samples of water were collected on board the vessels of the Sardinian Forestry Corps. Samplings were conducted at four coastal sites along orthogonal transects extending seaward from the coast, specifically designed to capture spatial variability across nearshore and offshore waters and to account for local differences in hydrodynamic conditions and anthropogenic pressure.

The manta trawl was equipped with a 330 μm mesh and a 25 × 50 cm mouth opening and was towed from the side of the vessel at an average speed of approximately 23 knots for 20 min. This sampling approach was intended to target the upper layer of the water column, where floating MPs are most likely to accumulate. A mechanical flowmeter installed at the net opening recorded the volume of water filtered during each tow, enabling MP concentrations to be expressed as items per cubic metre and thus allowing comparisons among stations.

At the end of each haul, the material retained in the cod-end was carefully rinsed into pre-cleaned containers using filtered seawater. All samples were then labeled with the relevant station information, including date, geographic coordinates, transect identity, and tow duration, and stored under cold conditions until laboratory processing.

Samples were transported to the laboratory and processed under controlled conditions. The collected material was first dried at room temperature and subsequently sieved to isolate the fraction of interest. MP particles were then visually sorted under a stereomicroscope based on morphological features (e.g., color, shape, and texture) and manually separated from the bulk.

The samples were kept in the laboratory for approximately 12 h during hydrogen peroxide digestion to remove plankton and residual organic matter. Once the organic material had been removed, the solution was filtered onto 100 mm sieve (Giuliani steel sieves).

Suspected MP particles were collected and stored for further spectroscopic analysis. Prior to analysis, all samples were handled using contamination control procedures, including the use of clean laboratory equipment and minimization of airborne particles.

To obtain a reference identification of the polymer composition, individual particles isolated from environmental samples were analyzed by Fourier-transform infrared (FTIR) spectroscopy. FTIR measurements were performed on single particles using a Nicolet iN10 MX infrared imaging microscope (Thermo Scientific, USA) operating in Attenuated Total Reflectance (ATR) mode. Spectra were acquired in the mid-infrared region (4000–675 cm^{-1}) with a spectral resolution of 8 cm^{-1}. To improve the signal-to-noise ratio, 64 scans were accumulated for each spectrum. Background spectra were collected prior to each measurement and automatically subtracted. Atmospheric compensation was applied to correct for contributions from H_2O and CO_2.

A total of 282 MP particles were analyzed across the four sampling sites, namely Castelsardo (25 MPs), Sinis (29 MPs), Teulada (24 MPs), and Capo Caccia (204 MPs). Based on the sampling configuration, the analyzed fragments were generally in the sub-millimetre to millimetre size range, typically from about 500 μm up to 1–2 mm. The distribution of polymer types for each site is reported in the Supporting Information (Section S3).

After FTIR identification, the particles from each sampling site were grouped to reconstruct representative mixed MP samples. Specifically, all fragments identified within each site were pooled together to obtain a single composite MP sample per location. These pooled samples were subsequently analyzed using the portable MicroNIR spectrometer under the same acquisition conditions adopted for the laboratory-prepared mixtures (Section 2.7).

2.6. Instrumentation and spectra acquisition

NIR spectra were collected using a MicroNIR OnSite-W spectrometer (Viavi Solutions, USA), a miniaturized and portable device suitable for non-destructive analysis of solid samples with minimal or no pretreatment. The instrument operates in the 910–1675 nm wavelength range, employing a Linear Variable Filter (LVF) as the dispersive element directly coupled to a 128-pixel InGaAs photodiode array. Each pixel corresponds to a specific wavelength defined by the thickness gradient of the LVF. Two integrated tungsten lamps serve as internal light sources, providing diffuse illumination of the sample. Spectra were acquired in diffuse reflectance mode with a nominal spectral resolution of 6.2 nm.

For laboratory-prepared samples (i.e., calibration and external validation sets), an aliquot of 100 mg was evenly spread on a clean metal plate, ensuring consistent optical thickness across samples.

In the case of environmental samples, the available amount of MP material obtained after FTIR identification and pooling was used without enforcing a fixed mass, due to the limited and variable quantity of recovered particles. The material from each site was evenly distributed on the sample holder to ensure homogeneous surface coverage during spectral acquisition.

In all cases, the NIR probe was positioned directly above the surface for spectral acquisition and 10 spectra were collected at random

positions on each sample to capture spatial heterogeneity and improve representativeness. Therefore, the calibration set comprised 89 samples (890 spectra), while the external validation sets consisted of 10 samples (100 spectra). Finally, the environmental sample set consisted of 4 samples (40 spectra).

2.7. Data analysis

The acquired NIR spectra were processed using a combination of different pre-processing techniques. Initially, each spectrum was cropped to the 963–1590 nm range to remove signal distortions caused by noisy regions and/or high variability that could compromise subsequent modelling [33]. Subsequently, standard normal variate (SNV) was applied to minimize additive scattering effects [34]. Furthermore, second derivatives were calculated to correct drift of spectra baseline and to enhance small intensity changes between mixtures resulting from variations in the polymer percentages [35]. Finally, data were mean-centered before modelling.

First, the calibration dataset was analyzed by means of Principal Component Analysis (PCA) [36], which is a well-known multivariate technique for exploratory data analysis. PCA projects the data in a multivariate space, defined by orthogonal principal components, which are linear combinations of the original variables. Outlier detection was performed exclusively on the calibration dataset at this stage, prior to model development.

Then, Partial Least Square (PLS) was used [37] for predicting the percentages of the polymers in the mixture from the NIR spectra. PLS is based on the projection of the predictor matrix X and the response vector Y into a space of lower dimensionality called Latent Variable (LV) space, by maximizing the covariance between them. As for PCA, these LVs are a combination of the original variables. The number of LVs for each model was selected on the basis of the cross-validation procedure. In this study, the percentage of each polymer in the mixture was modelled independently.

Finally, the proposed modelling strategy was evaluated using a double cross-validation procedure [38]. In particular, the calibration set was randomly divided into 4 folds. For any given sample, all of its ten spectra were constrained to be assigned exclusively to the same fold. During an iterative process, each fold was used as the test set, while the remaining folds were used to train a temporary PLS model. An internal cross-validation was performed within the temporary training set to select the optimal number of LVs. The resulting model was then used to predict the responses of the test set. This process was repeated until each fold was served once as the test set.

Subsequently, the models' predictive performances were evaluated against the two external validation sets described in **Sections 2.3** and **Section 2.4**. Figures of merit such as Coefficient of Determination (R^2) and Root Mean Squared Error (RMSE) were calculated for calibration, double cross-validation, and external validation procedures. Notably, these metrics were calculated using individual spectra to account for spectral variability and provide a more robust and demanding assessment, rather than using sample-averaged spectra. Since four PLS models were calculated (one for each polymer), figures of merit were calculated independently for each model.

All data analysis was performed by means of ad-hoc MATLAB functions based on the Principal Components Analysis toolbox [39] and the regression toolbox for MATLAB [40].

3. Results and discussion

3.1. Mechanical fragmentation and MP characterization

The use of mechanical fragmentation for producing true-to-life MP particles is increasingly recognized as a valuable approach, because it can better approximate the physical, morphological, and surface-textural heterogeneity typical of environmental MPs compared with pristine laboratory polymers [41,42]. Indeed, recent comparative studies have demonstrated that different cryogenic grinding or milling techniques yield MP fragments that differ significantly in their size distribution, shape, surface roughness, and internal structural properties (e.g., cracks, fissures) depending on the fragmentation method adopted [43–45]. These morphological and structural features influence critical physicochemical properties of MPs, including specific surface area, surface chemistry (e.g., oxidation, presence of functional groups), porosity, hydrophilicity/hydrophobicity, and mechanical strength, which, in turn, may strongly affect environmental behavior such as aggregation, settling, adsorption of contaminants, and degradation dynamics [46,47]. For example, mechanical fragmentation has been shown to increase surface area and introduce oxygen-containing functional groups (e.g., via cracking, surface oxidation), thereby potentially enhancing MP adsorption capacity for heavy metals or organic pollutants [44].

In this study, we applied a fragmentation protocol designed to mimic realistic environmental fragmentation (cryogenic embrittlement combined with mechanical milling / grinding) to generate an MP test material that captures a plausible level of heterogeneity in terms of polymer type, particle size distribution, and surface characteristics, consistent with what may be expected in field samples. A comprehensive physicochemical and morphological characterization of MPs produced using this protocol has been reported in previous studies [24,31,48]. This is crucial for the validation of spectroscopic methods combined with multivariate modelling, because these methods must cope with the spectral variability introduced by morphological and chemical heterogeneity.

3.2. NIR spectral characteristic bands

The NIR spectra of PP, PS, PE, and PET are shown in Fig. 1, with the interpretation of the most relevant bands provided in Table 1. The four polymers exhibit several distinct NIR features that make them identifiable. However, spectral overlap is also significant, which makes direct quantification in mixtures by means of univariate analysis unfeasible.

3.3. Exploratory analysis

The ten NIR spectra measured for each of the 89 calibration samples were organized in a data matrix with dimensions 890 rows (spectra) and 125 columns (wavelengths).

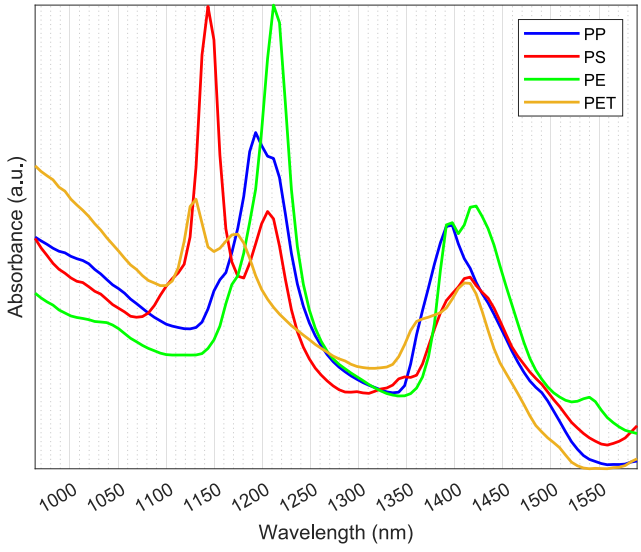

Fig. 1. NIR spectra of pure PP, PS, PE and PET. Spectra were preprocessed with SNV.

Table 1
Interpretation of the most characteristic NIR bands for the four polymers shown in Fig. 1, based on the information provided in [49,50]. (Assignments refer to dominant contributions; overlapping combination bands are expected in all regions.)

Polymer	Band (nm)	Interpretation
PP	1160–1205	2nd overtone of aliphatic C—H (mainly CH_3, CH_2)
PP	1205–1260	2nd overtone of CH_3 C—H stretching
PP	1350–1490	Combination bands and 1st overtone of CH_3/CH_2 C–H
PS	1120–1170	Higher overtones of aromatic C–H
PS	1170–1250	2nd overtone of aromatic and benzylic C–H
PS	1360–1490	Combination bands and 1st overtone of aromatic C–H
PE	1150–1260	2nd overtone of aliphatic CH_2 C–H
PE	1350–1400	Combination of CH stretching and CH_2 bending
PE	1400–1490	Combination bands and 1st overtone of CH_2 C–H
PE	1515–1560	Higher-order CH_2 combination / tail of 1st overtone
PET	1105–1145	Higher overtones of aromatic C—H (ring)
PET	1145–1200	2nd overtone of aromatic and CH_2 C–H
PET	1335–1385	Combination of C—H stretch and bending (aromatic + CH_2)
PET	1385–1490	Combination bands and 1st overtone of aromatic / CH_2 C–H

PCA was initially calculated considering only the 40 spectra of the pure polymers to evaluate the intrinsic variability among replicates under these specific NIR acquisition settings, as well as to assess the effects of the applied data pre-processing (spectral cropping, SNV, second derivative, and mean centering). The PCA scores and loadings are shown in Fig. 2: the four polymers are clearly clustered within the first two principal components, exhibiting distinctive spectral features highlighted in the loadings, which are in accordance with the characteristic bands shown in Fig. 1 for pure polymers. When looking at the score plot, PC1 explains spectral differences between PS (negative scores) and the rest of the polymers, while PC2 explains further differences between PP and PE, (positive scores) and PET (negative scores). However, spread of scores is also evident, reflecting the certain variability induced by physical measurements. Nevertheless, exploratory results provide a solid basis for subsequent quantitative analysis of the quaternary mixtures.

Afterwards, a further PCA was calculated on the entire dataset composed of 890 spectra, including all pure substances, binary, ternary, and quaternary mixtures to explore data referred to the different mixtures of polymers. Scores of the first three PCs are shown in Fig. 3, where samples have been colored according to the percentage of each polymer: ranging from 0% (dark blue) to 100% (wine red). The distribution of samples in the first three principal components correctly reflects the relative percentages of the different polymers in the mixtures, as indicated by the observed color spread, with spectra of pure substances located at the edges. Moreover, loadings of the first two PCs are shown in Fig. 4. These loadings are highly comparable to those derived from pure samples. This stability suggests that the intrinsic spectral fingerprints of the polymers are maintained within complex mixtures, providing a solid foundation for the subsequent multivariate quantitative analysis. Thus, the results demonstrate that the information contained in the spectral profiles enables the characterization of the mixtures according to the relative content of the individual polymers. In addition, an outlier diagnostic was conducted by means of Q residual versus Hotelling's T^2 metrics [36], with a total of 143 spectra removed from the dataset as potential outliers, as reported in **Fig. S4.a**. As shown in **Fig. S4.b**, the majority of outlier spectra are related to acquisition artifacts inherent to the measurement condition of portable NIR device and the distribution of MPs on the metal plate (e.g. signal instability, scattering effects, and variations in sample positioning). These outliers do not reflect the intrinsic physical heterogeneity of the microparticles, which would have

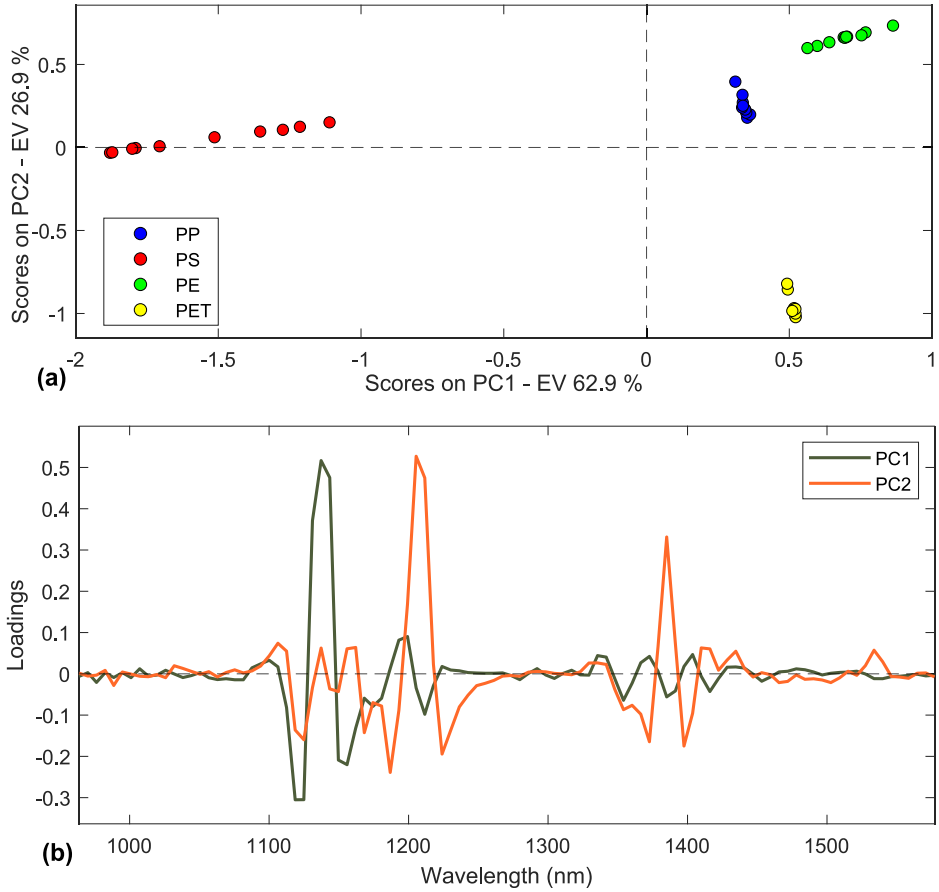

Fig. 2. Scores (a) and loadings (b) of the first two principal components for pure polymers.

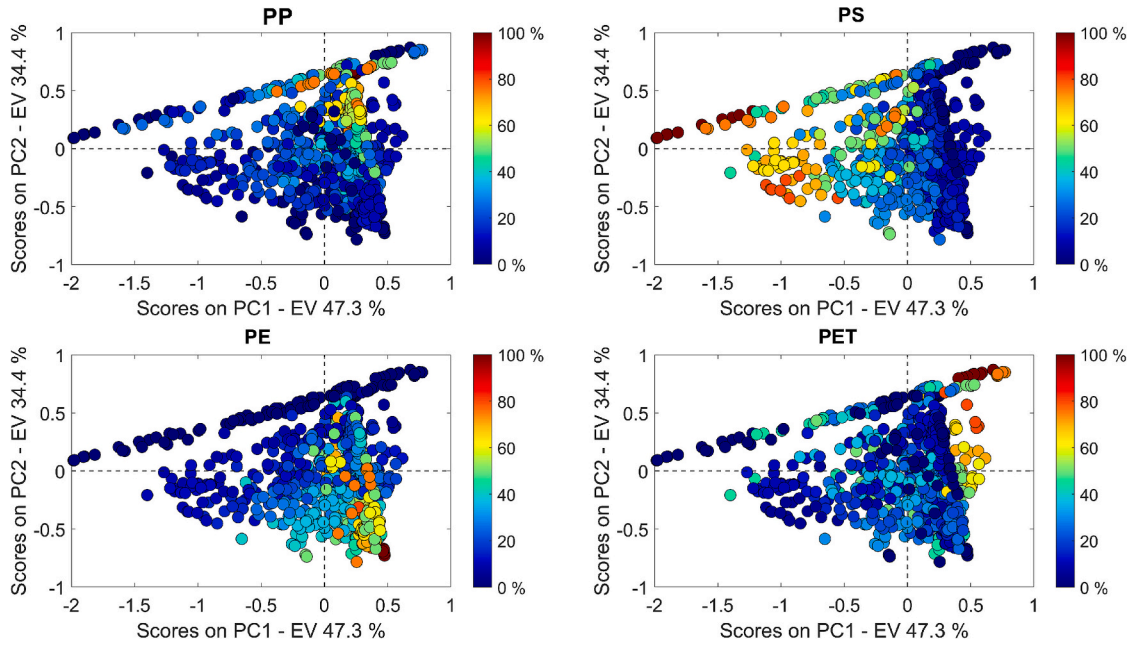

Fig. 3. Score plots of PC1 vs. PC2 based on the NIR spectra of polymer mixtures. Samples are colored according to the percentage of: (a) PP, (b) PS, (c) PE, and (d) PET, ranging from 0% (dark blue) to 100% (wine red). (For interpretation of the references to color in this figure legend, the reader is referred to the web version of this article.)

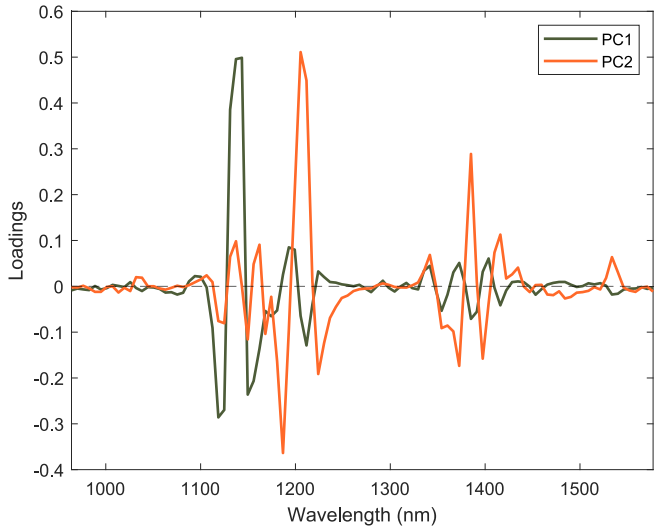

Fig. 4. PCA loadings of PC1 (dark green) and PC2 (orange). (For interpretation of the references to color in this figure legend, the reader is referred to the web version of this article.)

otherwise improved the model's predictive quality, and thus removed and not used for modelling.

3.4. Quantification of MP composition

Four independent PLS regression models were subsequently calibrated to model the percentage of each polymer in the mixtures, using the remaining 747 spectra after outlier diagnosis. Therefore, the final dataset used for modelling consisted of 40 spectra of pure substances, 76 binary-mixture spectra, 94 ternary-mixture spectra, and 537 quaternary-mixture spectra. Using multiple spectra from each sample instead of the average spectrum makes it possible to capture the intrinsic variability associated with portable devices for in-situ measurements, where small variations in the spectral signal are expected when acquiring spectra from different points of the sample holder.

Table 2 collects figures of merit for regression performances. While model performance slightly differed among polymers, the maximum prediction error (RMSE) for the double cross validation procedure was 11.1% for PE model. Such performance can be regarded as satisfactory and therefore supports the proposed modelling strategy for the quantitative prediction of quaternary mixtures, particularly considering the use of a portable NIR device for in-situ measurements, where a certain degree of variability is expected.

In order to understand which spectral information determines the quantification of each polymer, PLS regression coefficients were analyzed, as shown in Fig. 5.

As observed, the absolute values of the regression coefficients indicate that some wavelengths have major contributions. However, the quantification relies on the combined information from all wavelengths, not only on the most influential ones. With the exception of the PET model, where 1125 nm stands out as the most influential wavelength, no single wavelength appears to dominate in the other models, aside from minor exceptions around 1125 nm, 1200 nm, 1390–1420 nm, and 1385 nm. As direct interpretation of NIR bands becomes more challenging when derivative pre-processing is applied, readers are referred to Fig. 1, where spectra of pure polymers are shown using only SNV as pre-processing. The wavelength at 1125 nm, whose coefficient was particularly relevant for the PS and PET models, corresponds to the region where one of the main bands of PS partially overlaps with one of the PET peaks. Moreover, 1200 nm corresponds exactly to the point where one of

Table 2
Regression performance of the individual PLS models: coefficient of determination (R^2) and root mean squared error in % (RMSE) in calibration and double cross-validation.

	R^2		RMSE	
	Calibration	Double cross-validation	Calibration	Double Cross-validation
PP	0.88	0.84	7.9	9.17
PS	0.86	0.78	8.2	10.31
PE	0.85	0.76	8.7	11.10
PET	0.82	0.78	8.5	9.41

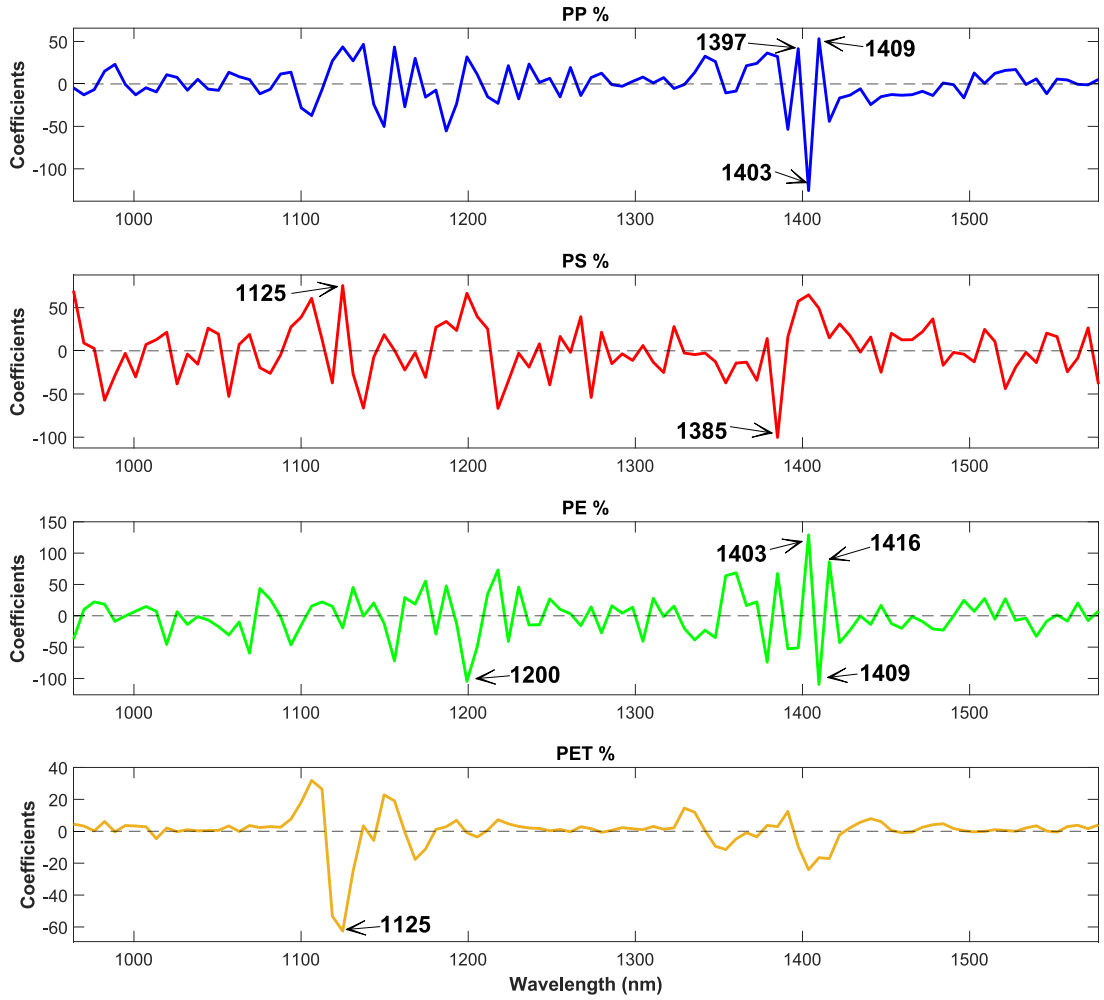

Fig. 5. PLS coefficients for (a) PP, (b) PS, (c) PE and (d) PET. Variables with high absolute coefficient values are labeled for model interpretation.

the main bands of PP, PE and PS overlaps, with PET not presenting any band close. In contrast, the 1390–1420 nm region, which contains several wavelengths with large coefficients, appears fundamental particularly for PP and PE models, although bands of all four polymers overlap in this very rich region. It is worth noting that the right interpretation of important bands must consider that derivative pre-processing emphasizes subtle spectral features. As a result, additional information useful for quantification may be highlighted, even if such features are not evident in spectra that have not been processed with derivatives. However, it is worth mentioning that a direct interpretation of PLS coefficients following second-derivative pre-processing requires careful consideration, as this transformation significantly alters the spectral shape [51]. Specifically, the second derivative effectively inverts the original absorbance bands, meaning that a peak in the raw spectrum appears as a local minimum in the processed data. Consequently, the resulting PLS coefficients correspond to the curvature of the spectral features rather than their absolute intensity.

3.5. *Assessment of true-to-life generalizability and potential interferents*

To explore the possible limitations of the proposed models when analyzing spectra of mixtures prepared with different true-to-life samples and in presence of interferents, two additional sets of samples (with and without addition of interferents) were used to further validate the PLS regression models. The predictions obtained for the new true-to-life samples before and after the addition of interferents are reported in **Table S3** and **Table S4**, respectively. Figures of merit (R^2 and RMSE) shown in Fig. 6 and Fig. 7 are calculated with respect to the predictions based on the individual spectra of the external validation set. However, given the large number of predicted spectra, only the average experimental versus predicted values are shown in these figures for clarity.

As observed, in the external validation set without interferents (Fig. 6) the models performed better than expected, with RMSE values comparable to those obtained during internal validation (Table 2). Moreover, with few exceptions, the standard deviation was relatively low, indicating that the models remain stable despite small variations in the NIR signal when different spectra of the sample are acquired.

When predicting the external validation set spiked with interferents (Fig. 7), RMSE values increase compared to the prediction of the same samples without added interferents. Significant variability was observed even between replicates of the same contaminant-mixture combination, likely due to NIR acquisition at different points of the heterogeneous metal plate. Consequently, prediction error for the PP and PS models slightly exceeded those observed during internal validation, while PE and PET were associated with similar RMSE (Table 2), suggesting that these polymers are less affected by this particular combination of interferents.

It is worth noting that, although prediction errors increased moderately, experiments performed on spiked samples with environmentally relevant interferents, provide valuable insight into the behavior of NIR-based quantitative models under realistic conditions. In this study, the interferents intentionally covered a broad spectrum of chemical and morphological classes, namely rigid polymers (PVC, PA66), semi-crystalline biodegradable polymers (PLA), natural fibres rich in O—H

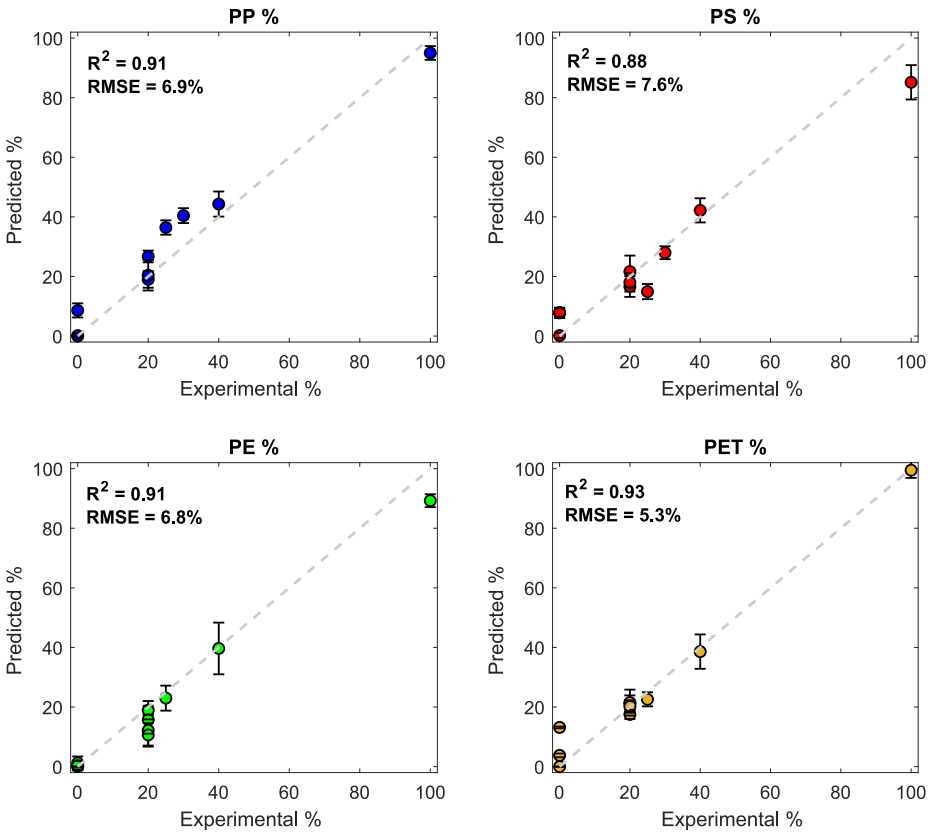

Fig. 6. Experimental vs. predicted % for samples included in the external validation set. Regression metrics are calculated by considering each spectrum as an independent observation, whereas only mean predicted value is plotted for clarity. Error bars are calculated as ± standard deviation of all the replicate spectra.

and N—H groups (cotton, silk), vegetal material with heterogeneous lignocellulosic signatures, and inorganic minerals such as $CaCO_3$, thus reproducing many of the complex components commonly found in field samples.

It is worth mentioning that the varying susceptibility of these polymers to matrix effects can be attributed to the level of spectral selectivity provided by their diagnostic bands. While PP and PE share similar aliphatic C—H overtone structures, the PLS coefficient (Fig. 5) reveals that the models exploit distinct features for each MP. For instance, the PE model relies on sharp features at 1403 and 1409 nm, whereas the PP model is heavily influenced by a specific band at 1385 nm. The higher RMSE for PP suggests that its primary diagnostic regions suffer from greater spectral overlapping more significantly with the broad absorption signatures of environmental interferents. Conversely, PET demonstrates the greatest resilience to matrix effects. Despite PS having a higher aromatic density, the PET model utilizes a more unique 'fingerprint' characterized by high-magnitude coefficients (e.g., the 1200 nm region and the 1403–1416 nm triplet). This enhanced robustness likely stems from the presence of carbonyl overtones and specific aromatic arrangements in PET that remain resolvable even against the complex NH- and OH- signatures of natural fibres and vegetal material.

Additionally, the variability observed among replicates of the same interferent-contaminated mixture indicates that sample heterogeneity and physical measurements contribute to prediction uncertainty, due to the local scattering effects, particles packing and micro-textural variations.

3.6. Application to real environmental samples

To evaluate the model's generalizability beyond controlled laboratory conditions, the quantification strategy was applied to four real environmental samples collected from coastal sites in Sardinia, Italy.

For each site, MP particles were first individually identified by FTIR spectroscopy, generating a particle-resolved reference dataset. Subsequently, all identified particles from each sampling location were pooled to reconstruct representative mixed MP samples, which were then analyzed using the portable NIR spectrometer under the same conditions adopted for laboratory-prepared mixtures. This approach enabled a direct comparison between NIR predictions and FTIR-derived reference compositions for each site.

Experimental and predicted % of MPs are collected in **Table 3**. The prediction performance yielded RMSE of 11% (PP), 15% (PS), 18% (PE), and 13% (PET), with an overall average RMSE of 14.3%. While these values are slightly higher than those achieved during laboratory validation in the presence of interferences (Fig. 7), the accuracy remains satisfactory considering the inherent complexity of "unknown" environmental matrices. Unlike synthetic mixtures, real samples contain polymers with diverse degradation histories and a higher load of unpredictable organic and inorganic interferents.

Additionally, variability in polymer distribution among the investigated sites (see **Table 3** and Supporting Information, **Fig. S2**) further contributes to the complexity of the system, as different mixtures may emphasize or suppress specific spectral features depending on the dominant polymer classes.

In the context of on-site monitoring, these results demonstrate that the portable NIR approach provides a reliable semi-quantitative screening tool. The trade-off between a moderate increase in uncertainty and the benefits of a rapid, cost-effective, and non-destructive assessment is well-justified for first-tier environmental surveys where high-throughput data is prioritized over the precision of laboratory-bound reference methods.

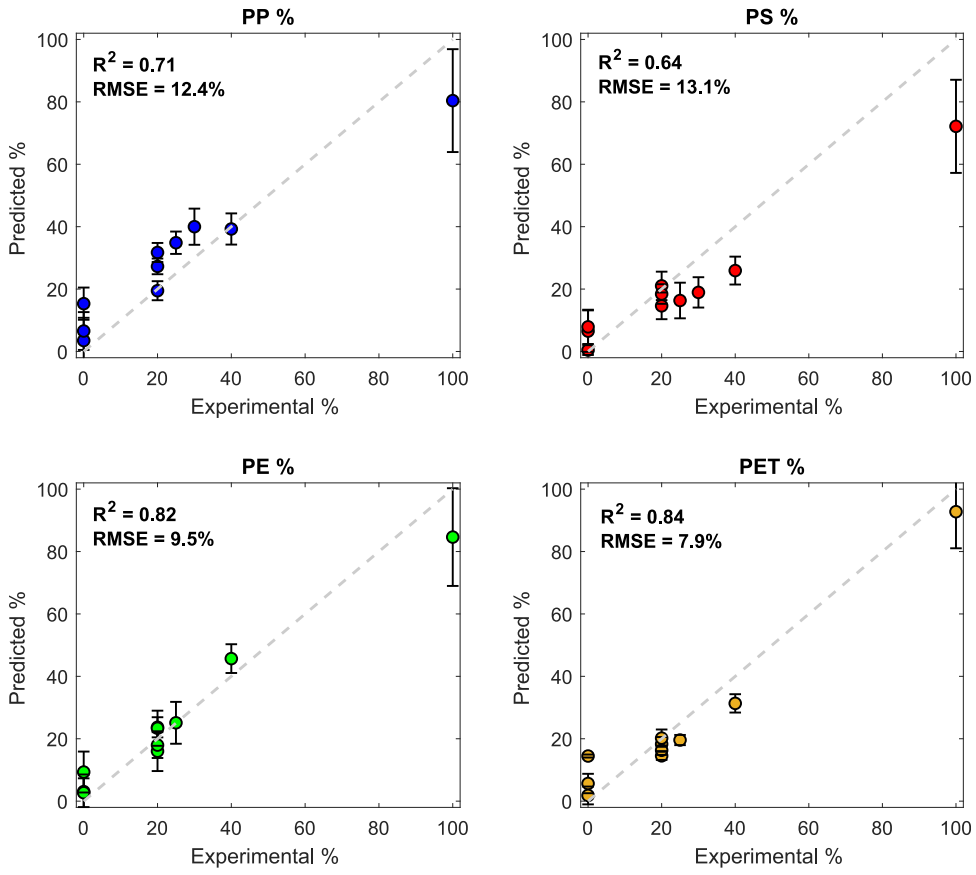

Fig. 7. Experimental vs. predicted % for samples included in the external validation set spiked with interferents. Regression metrics are calculated by considering each spectrum as an independent observation, whereas only mean predicted value is plotted for clarity. Error bars are calculated as ± standard deviation of all the replicate spectra.

Table 3
Experimental and predicted % of microplastics in environmental samples.

	experimental %				predicted %			
samples	PP	PS	PE	PET	PP	PS	PE	PET
Castelsardo	12	0	36	0	19	19	58	14
Sinis	10	4	72	0	23	9	60	13
Teulada	8	0	71	0	19	16	47	14
C. Caccia	6	1	74	0	20	16	61	12

4. Conclusions

In this study, a portable NIR spectroscopic approach combined with multivariate regression was developed and evaluated for the quantification of four polymers (PP, PS, PE, and PET) in complex MP mixtures prepared under realistic laboratory conditions. By adopting a true-to-life fragmentation procedure, the resulting MPs reproduced the morphological and chemical variability typically encountered in environmental samples, thereby providing a robust basis for model calibration.

The proposed PLS regression modelling approach demonstrated satisfactory predictive ability, with RMSE in double cross-validation below 11.1% for all polymers. A further external validation of these models was performed by preparing mixtures of polymers selected from different commercial products to ensure chemical and morphological variability with respect to the calibration set. In this case, the maximum RMSE achieved was 7.6% for PS model These results confirmed the applicability of the models, which maintained accuracy levels comparable to those achieved during double cross-validation.

When the same mixtures of the external validation set were spiked with a wide range of interferents, prediction errors slightly increased, reflecting the spectral complexity introduced by other plastic types and non-plastic materials. Nevertheless, the models retained a meaningful predictive capacity, with PP and PS being more affected by matrix interferences in the tested conditions (RMSE equal to 12.4% and 13.1%, respectively). These results highlight the potential of portable NIR spectroscopy for quantitative MP analysis in heterogeneous matrices.

Moreover, when the models were applied to real environmental samples, the RMSE ranged between 11% and 18%. As expected, the average RMSE increased, reflecting the inherent complexity of real-world matrices compared to controlled laboratory mixtures. Considering the intrinsic complexity of environmental matrices and the practical advantages of portable NIR instrumentation for in situ prescreening analysis, the achieved performance can be regarded as satisfactory. Thus, the proposed modelling strategy is aimed at preliminary assessment and screening purposes. Although matrix effects remain a critical challenge, especially in the presence of interferents, this work represents a significant step toward the development of operational, cost-effective methods for on-site MP monitoring. Future efforts should focus on expanding calibration datasets, incorporating a broader diversity of environmental interferents in the modelling approach, and improving spectral acquisition strategies to further enhance model robustness in real-world scenarios.

Furthermore, the implementation of a hierarchical modelling architecture could be explored to refine prediction reliability. In such a framework, a preliminary qualitative classification step would first predict the presence or absence of a specific polymer, followed by quantitative PLS1 regression only for confirmed samples. This two-stage approach could better address the inherent uncertainty of regression near the detection limit (±RMSE) and provide a more sophisticated workflow for handling complex environmental matrices.

CRediT authorship contribution statement

Enmanuel Cruz Muñoz: Writing – original draft, Methodology, Investigation, Data curation, Conceptualization. **Claudio Marchesi:** Methodology, Investigation, Conceptualization. **Mario Rigo:** Methodology, Investigation. **Sundus Ali:** Methodology, Investigation. **Laura Eleonora Depero:** Funding acquisition. **Giuseppe Andrea de Lucia:** Funding acquisition, Investigation. **Andrea Camedda:** Investigation. **Silvia Prati:** Investigation, Data curation. **Davide Ballabio:** Writing – review & editing, Methodology, Data curation. **Giorgia Sciutto:** Writing – review & editing, Writing – original draft, Methodology, Funding acquisition, Data curation, Conceptualization. **Stefania Federici:** Writing – review & editing, Writing – original draft, Methodology, Funding acquisition, Conceptualization.

Declaration of competing interest

The authors declare that they have no known competing financial interests or personal relationships that could have appeared to influence the work reported in this paper.

Acknowledgments

This article is based upon work from COST Action CA20101 Plastics monitoring detectiOn RemedIaTion recovery, PRIORITY, supported by COST (European Cooperation in Science and Technology, www.cost.eu). S.F. and M.R. acknowledge the Italian Ministry of University and Research (Research program "Research Projects of National Relevance, PRIN 2022") and the project "PLASTACTS - Assessment of nano/microplastics impacts", 202293AX2L, CUP D53D23009050001. G.S. and S.P. acknowledge the financial support from Italian Ministry of University and Research, Research program Research Projects of National Relevance, PRIN PNRR 2022 (project "DIORAMA - A deep dive into the study of microplastics in aqueous matrices", P20227N5YZ_001, CUP J53D23014500001). C.M., S.F., and L.E.D. acknowledge PON "R&I" 2014-2020: SIRIMAP—SIstemi di Rilevamento dell'Inquinamento MArino da Plastiche e successivo recupero-riciclo (No. ARS01_01183) CUP D86C18000520008.

Appendix A. Supplementary data

Supplementary data to this article can be found online at https://doi.org/10.1016/j.microc.2026.118027.

Data availability

Data will be made available on request.

References

[1] International Organization for Standardization, ISO/TR 21960:2020 Plastics-Environmental aspects-State of knowledge and methodologies, 2020.
[2] Sapea, A scientific perspective on Micro-plastics in nature and society, 2019.
[3] R.C. Thompson, W. Courtene-Jones, J. Boucher, S. Pahl, K. Raubenheimer, A. A. Koelmans, Twenty years of microplastic pollution research—what have we learned? Science 386 (2024) https://doi.org/10.1126/SCIENCE.ADL2746;SUBPAGE:STRING:FULL.
[4] C.M. Rochman, T. Hoellein, The global odyssey of plastic pollution, Science 368 (2020) 1184–1185, https://doi.org/10.1126/SCIENCE.ABC4428.
[5] M. MacLeod, H.P.H. Arp, M.B. Tekman, A. Jahnke, The global threat from plastic pollution, Science 373 (2021) 61–65, https://doi.org/10.1126/SCIENCE.ABG5433.
[6] A. Stubbins, K.L. Law, S.E. Muñoz, T.S. Bianchi, L. Zhu, Plastics in the Earth system, Science 373 (2021) 51–55, https://doi.org/10.1126/SCIENCE.ABB0354.
[7] N.B. Hartmann, T. Hüffer, R.C. Thompson, M. Hassellöv, A. Verschoor, A. E. Daugaard, S. Rist, T. Karlsson, N. Brennholt, M. Cole, M.P. Herrling, M.C. Hess, N.P. Ivleva, A.L. Lusher, M. Wagner, Are we speaking the same language? Recommendations for a definition and categorization framework for plastic debris, Environ. Sci. Technol. 53 (2019) 1039–1047, https://doi.org/10.1021/acs.est.8b05297.
[8] J. Song, C. Wang, G. Li, Defining primary and secondary microplastics: a connotation analysis, ACS ES T Water 4 (2024) 2330–2332, https://doi.org/10.1021/ACSESTWATER.4C00316.
[9] J. Boucher, D. Friot, Primary microplastics in the oceans: A global evaluation of sources. Primary microplastics in the oceans: a global evaluation of sources, 2017, https://doi.org/10.2305/IUCN.CH.2017.01.EN.
[10] S. Amberg, D.M. Mitrano, Exploring the essential use concept for primary microplastics regulation in the EU, Environ. Sci. Technol. 59 (2025) 7799–7809, https://doi.org/10.1021/ACS.EST.4C10830.
[11] H.-C. Lu, S. Ziajahromi, P.A. Neale, F.D.L. Leusch, A systematic review of freshwater microplastics in water and sediments: recommendations for harmonisation to enhance future study comparisons, Sci. Total Environ. 781 (2021), https://doi.org/10.1016/j.scitotenv.2021.146693.
[12] V. Hidalgo-Ruz, L. Gutow, R.C. Thompson, M. Thiel, Microplastics in the marine environment: a review of the methods used for identification and quantification, Environ. Sci. Technol. 46 (2012) 3060–3075, https://doi.org/10.1021/es2031505.
[13] A. Käppler, D. Fischer, S. Oberbeckmann, G. Schernewski, M. Labrenz, K. J. Eichhorn, B. Voit, Analysis of environmental microplastics by vibrational microspectroscopy: FTIR, Raman or both? Anal. Bioanal. Chem. 408 (29) (2016) 8377–8391, https://doi.org/10.1007/S00216-016-9956-3.
[14] International Organization for Standardization, ISO 16094-2 water quality — analysis of microplastic in water. Part 2: vibrational spectroscopy methods for waters with low content of suspended solids including drinking water, 2025.
[15] D. Schymanski, B.E. Oßmann, N. Benismail, K. Boukerma, G. Dallmann, E. von der Esch, D. Fischer, F. Fischer, D. Gilliland, K. Glas, T. Hofmann, A. Käppler, S. Lacorte, J. Marco, M. El Rakwe, J. Weisser, C. Witzig, N. Zumbülte, N.P. Ivleva, Analysis of microplastics in drinking water and other clean water samples with micro-Raman and micro-infrared spectroscopy: minimum requirements and best practice guidelines, Anal. Bioanal. Chem. 413 (24) (2021) 5969–5994, https://doi.org/10.1007/S00216-021-03498-Y.
[16] Y.K. Song, S.H. Hong, S. Eo, W.J. Shim, A comparison of spectroscopic analysis methods for microplastics: manual, semi-automated, and automated fourier transform infrared and raman techniques, Mar. Pollut. Bull. 173 (2021) 113101, https://doi.org/10.1016/J.MARPOLBUL.2021.113101.
[17] M. Rani, S. Ducoli, S. Federici, L.E. Depero, Influx of near-infrared technology in microplastic community: a bibliometric analysis, Microplastics 2 (2023) 107–121, https://doi.org/10.3390/microplastics2010008.
[18] M. Rani, C. Marchesi, S. Federici, G. Rovelli, I. Alessandri, I. Vassalini, S. Ducoli, L. Borgese, A. Zacco, F. Bilo, E. Bontempi, L.E. Depero, Miniaturized near-infrared (MicroNIR) spectrometer in plastic waste sorting, Materials 12 (2019), https://doi.org/10.3390/ma12172740.
[19] K.B. Bec, J. Grabska, F. Pfeifer, H.W. Siesler, C.W. Huck, Rapid on-site analysis of soil microplastics using miniaturized NIR spectrometers: key aspect of instrumental variation, J. Hazard. Mater. 480 (2024) 135967, https://doi.org/10.1016/J.JHAZMAT.2024.135967.
[20] J. Grabska, K.B. Beć, C.W. Huck, Current and future applications of IR and NIR spectroscopy in ecology, environmental studies, wildlife and plant investigations, Compr. Anal. Chem. 98 (2022) 45–76, https://doi.org/10.1016/BS.COAC.2020.08.002.
[21] S. Piarulli, G. Sciutto, P. Oliveri, L. Airoldi, Rapid and direct detection of small microplastics in aquatic samples by a new near infrared hyperspectral imaging (NIR-HSI) method, Chemosphere 260 (2020), https://doi.org/10.1016/j.chemosphere.2020.127655.
[22] C. Vidal, C. Pasquini, A comprehensive and fast microplastics identification based on near-infrared hyperspectral imaging (HSI-NIR) and chemometrics, Environ. Pollut. 285 (2021), https://doi.org/10.1016/j.envpol.2021.117251.
[23] C. Pasquini, Near infrared spectroscopy: a mature analytical technique with new perspectives – a review, Anal. Chim. Acta 1026 (2018) 8–36, https://doi.org/10.1016/J.ACA.2018.04.004.
[24] C. Marchesi, M. Rani, S. Federici, I. Alessandri, I. Vassalini, S. Ducoli, L. Borgese, A. Zacco, A. Núñez-Delgado, E. Bontempi, L.E. Depero, Quantification of ternary microplastic mixtures through an ultra-compact near-infrared spectrometer coupled with chemometric tools, Environ. Res. 216 (2023), https://doi.org/10.1016/j.envres.2022.114632.
[25] A. Asrafy, L. Akter, M.N. Islam, M. Billah, S.T. Arafat, M.M. Rahman, S.M. Rahman, Microplastics pollution: a brief review of its source and abundance in different aquatic ecosystems, J. Hazardous Mater. Adv. 9 (2023) 100215, https://doi.org/10.1016/j.hazadv.2022.100215.
[26] M. Hoseini, T. Bond, Predicting the global environmental distribution of plastic polymers, Environ. Pollut. 300 (2022) 118966, https://doi.org/10.1016/j.envpol.2022.118966.
[27] L. Wang, B. Zu, Q. Yang, J. Guo, J. Li, Sources, distribution, and environmental effects of microplastics: a systematic review, RSC Adv. 13 (2023) 15566–15574, https://doi.org/10.1039/D3RA02169F.
[28] R. Geyer, J.R. Jambeck, K.L. Law, Production, use, and fate of all plastics ever made, Sci. Adv. 3 (2017) doi:10.1126/SCIADV.1700782;PAGE:STRING:ARTICLE/CHAPTER.
[29] Europe P, EPRO, Plastics - the Facts 2019, 2019.
[30] L. Cai, Z. Yang, Z. Shi, X. Zhang, J. Li, L. Han, Influence of soil types with different soil-forming process on the qualitative and quantitative detection of microplastics by near-infrared spectroscopy, J. Environ. Sci. (2025), https://doi.org/10.1016/J.JES.2025.11.056.
[31] S. Ducoli, M. Rani, C. Marchesi, M. Speziani, A. Zacco, G. Gavazzi, S. Federici, L. E. Depero, Comparison of different fragmentation techniques for the production of true-to-life microplastics, Talanta 283 (2025), https://doi.org/10.1016/j.talanta.2024.127106.

[32] A. Sbrana, T. Valente, J. Bianchi, S. Franceschini, R. Piermarini, F. Saccomandi, A. G. de Lucia, A. Camedda, M. Matiddi, C. Silvestri, From inshore to offshore: distribution of microplastics in three italian seawaters, Environ. Sci. Pollut. Res. 30 (2023) 21277–21287, https://doi.org/10.1007/s11356-022-23582-9.
[33] Rinnan Åsmund, Berg F. Van Den, S.B. Engelsen, Review of the most common pre-processing techniques for near-infrared spectra, TrAC Trends Anal. Chem. 28 (2009) 1201–1222, https://doi.org/10.1016/j.trac.2009.07.007.
[34] R.J. Barnes, M.S. Dhanoa, S.J. Lister, Standard normal variate transformation and De-trending of near-infrared diffuse reflectance spectra, Appl. Spectrosc. 43 (1989) 772–777, https://doi.org/10.1366/0003702894202201.
[35] A. Savitzky, M.J.E. Golay, Smoothing and differentiation of data by simplified least squares procedures, Anal. Chem. 36 (1964) 1627–1639, https://doi.org/10.1021/ac60214a047.
[36] R. Bro, A.K. Smilde, Principal component analysis. Anal, Methods 6 (2014) 2812–2831, https://doi.org/10.1039/C3AY41907J.
[37] S. Wold, M. Sjöström, L. Eriksson, PLS-regression: a basic tool of chemometrics, Chemom. Intell. Lab. Syst. 58 (2001) 109–130, https://doi.org/10.1016/S0169-7439(01)00155-1.
[38] P. Filzmoser, B. Liebmann, K. Varmuza, Repeated double cross validation, J. Chemom. 23 (2009) 160–171, https://doi.org/10.1002/cem.1225.
[39] D. Ballabio, A MATLAB toolbox for principal component analysis and unsupervised exploration of data structure, Chemom. Intell. Lab. Syst. 149 (2015) 1–9, https://doi.org/10.1016/j.chemolab.2015.10.003.
[40] V. Consonni, G. Baccolo, F. Gosetti, R. Todeschini, D. Ballabio, A MATLAB toolbox for multivariate regression coupled with variable selection, Chemom. Intell. Lab. Syst. 213 (2021) 104313, https://doi.org/10.1016/j.chemolab.2021.104313.
[41] K. Altmann, L. Wimmer, V. Alcolea-Rodriguez, T. Waniek, V. Wachtendorf, K. Matzdorf, D. Ciornii, P. Fengler, F. Milczewski, I. Otazo-Aseguinolaza, M. Ferrer, M.A. Bañares, R. Portela, L.A. Dailey, Quality-by-design and current good practices for the production of test and reference materials for micro- and nano-plastic research, J. Hazard. Mater. 497 (2025) 139595, https://doi.org/10.1016/J.JHAZMAT.2025.139595.
[42] D. Ciornii, V.D. Hodoroaba, N. Benismail, A. Maltseva, J.F. Ferrer, J. Wang, R. Parra, R. Jézéquel, J. Receveur, D. Gabriel, A. Scheitler, C. van Oversteeg, J. Roosma, A. van Renesse van Duivenbode, T. Bulters, M. Zanella, A. Perini, F. Benetti, D. Mehn, G. Dierkes, M. Soll, T. Ishimura, M. Bednarz, G. Peng, L. Hildebrandt, M. Peters, S.K. Kim, J. Türk, F. Steinfeld, J. Jung, S. Hong, E.J. Kim, H.W. Yu, S. Klockmann, C. Krafft, J. Süssmann, S. Zou, A. ter Halle, A. M. Giovannozzi, A. Sacco, M. Fadda, M. Putzu, D.H. Im, N. Nhlapo, P. Carrillo-Barragán, N. Schmidt, D. Herzke, A. Gomiero, A. Jaén-Gil, D.J.E. Cabanes, M. Doedt, V. Cardoso, A. Schmitz, M. Hawly, H. Mo, J. Jacquin, A. Mechlinski, G. A. Adediran, J. Andrade, S. Muniategui-Lorenzo, A. Ramsperger, M.G.J. Löder, C. Laforsch, T. Cirkovic Velickovic, D. Fabbri, I. Coralli, S. Federici, B.M. Scholz-Böttcher, J. la Nasa, G. Biale, C. Rauert, E.D. Okoffo, A. Undas, L. An, V. Wachtendorf, P. Fengler, K. Altmann, Interlaboratory comparison reveals state of the art in microplastic detection and quantification methods, Anal. Chem. 97 (2025) 8719–8728, https://doi.org/10.1021/ACS.ANALCHEM.4C05403.
[43] I. Chubarenko, I. Efimova, M. Bagaeva, A. Bagaev, I. Isachenko, On mechanical fragmentation of single-use plastics in the sea swash zone with different types of bottom sediments: insights from laboratory experiments, Mar. Pollut. Bull. 150 (2020) 110726, https://doi.org/10.1016/j.marpolbul.2019.110726.
[44] Y. Yan, Y. Yu, J. Sima, C. Geng, J. Yang, Aging behavior of microplastics accelerated by mechanical fragmentation: alteration of intrinsic and extrinsic properties, Environ. Sci. Pollut. Res. 30 (2023) 90993–91006, https://doi.org/10.1007/s11356-023-28736-x.
[45] B.K. Pramanik, S.K. Pramanik, S. Monira, Understanding the fragmentation of microplastics into nano-plastics and removal of nano/microplastics from wastewater using membrane, air flotation and nano-ferrofluid processes, Chemosphere 282 (2021) 131053, https://doi.org/10.1016/j.chemosphere.2021.131053.
[46] C. Sorasan, C. Edo, M. González-Pleiter, F. Fernández-Piñas, F. Leganés, A. Rodríguez, R. Rosal, Ageing and fragmentation of marine microplastics, Sci. Total Environ. 827 (2022) 154438, https://doi.org/10.1016/j.scitotenv.2022.154438.
[47] S. Ducoli, C. Marchesi, M. Rigo, A. Zacco, E. Caianiello, R. Castaldo, M. Cocca, S. Federici, L.E. Depero, Developing environmentally relevant test materials for microplastic research through UV-induced photoaging, J. Hazardous Mater. Adv. 20 (2025) 100905, https://doi.org/10.1016/J.HAZADV.2025.100905.
[48] S. Ducoli, M. Rani, C. Marchesi, M. Speziani, A. Zacco, G. Gavazzi, S. Federici, L. E. Depero, Comparison of different fragmentation techniques for the production of true-to-life microplastics, Talanta 283 (2025) 127106, https://doi.org/10.1016/J.TALANTA.2024.127106.
[49] D.A. Burns, E.W. Ciurczak, Handbook of Near-Infrared Analysis, CRC Press, 2007.
[50] J. Workman Jr., L. Weyer, Practical Guide and Spectral Atlas for Interpretive Near-Infrared Spectroscopy, CRC Press, 2012.
[51] P. Oliveri, C. Malegori, R. Simonetti, M. Casale, The impact of signal pre-processing on the final interpretation of analytical outcomes – a tutorial, Anal. Chim. Acta 1058 (2019), https://doi.org/10.1016/j.aca.2018.10.055.